Appl. Phys. A 56, 87–90 (1993)

Applied Physics A Solids and Surfaces

Rapid Communications

Thermal Diffusivity Measurements of Natural and Isotopically Enriched Diamond by Picosecond Infrared Transient Grating Experiments

A. Tokmakoff[1], **W. F. Banholzer**[2], **M. D. Fayer**[1]

[1] Department of Chemistry, Stanford University, Stanford, CA 94305, USA (Fax: +1-415/723-4817)
[2] GE Superabrasives, 6325 Huntley Rd., Worthington, OH 43085, USA

Received 15 October 1992/Accepted 10 November 1992

Abstract. The thermal diffusivity of natural abundance and isotopically enhanced, synthetic, diamond crystals have been directly measured by picosecond infrared transient grating experiments operating on a microscopic distance scale. Transient gratings do not require contact to the sample, and are not limited by sample size, or complicated modeling or fitting of the data. Single crystal type-IIA diamond samples with natural abundance of ^{12}C (98.9%) and enriched ^{12}C isotopic abundance (99.9%) gave diffusivity constants of 7.8 cm^2/s and 12.0 cm^2/s, respectively, at room temperature. These results confirm previous measurements of a 50% increase in the thermal conductivity of isotopically enhanced diamond. Variations in the thermal diffusivity of up to 50% were observed from point to point in both samples.

PACS: 66.10.Cb, 62.65.+k, 42.65.Ft, 42.65.Ky

Diamond is a material of considerable interest for its thermal and mechanical properties. The unusually high thermal conductivity of diamond, its hardness, and the improvement in the growth of CVD films make it a candidate for heat sinks and substrates in electronic devices. In addition, the thermal conductivity of natural abundance versus isotopically enriched diamond is of great interest in light of reports of large enhancements in thermal conductivity in ^{12}C enriched type-IIA diamonds. The unusually high thermal conductivities of isotopically enriched diamond are reported to exceed the already great thermal conductivity of natural abundance diamond (98.9% ^{12}C) by 50% [1, 2].

The measurement of extremely large thermal conductivities, such as those of diamond, is difficult. Traditional steady-state measurement techniques require contact with the sample, and are limited by the size of the sample [3, 4]. Modulated laser heating techniques require complex models describing the phase or amplitude of thermal waves [1, 5]. Measurements of transient infrared signals after pulsed heating, have provided the most direct measurements to date, but are also limited by the size of the sample and the description of the thermal wave in most cases [6, 7].

In this report, we demonstrate the measurement of thermal conductivity on natural and isotopically enriched type-IIA diamond using picosecond infrared transient grating experiments. To our knowledge, these are the first nonlinear experiments conducted with picosecond infrared pulses. The transient grating is an entirely optical technique; it is non-invasive, direct, and requires no modeling. Sample size limitations are dictated only by the laser beam spot size. The experiment directly probes the bulk of the sample on a small distance scale and is not influenced by surface effects. In addition, this technique has internal consistency checks that allow verification of the results. A transient grating measurement gives the thermal diffusivity, α, which can be related to the thermal conductivity, k, by $k = \alpha \varrho C_p$, where ϱ is the density of the sample and C_p is the heat capacity.

1 Experimental Procedures

Transient gratings have been used to measure numerous dynamic phenomena, including thermal diffusion [8], excitation transport in crystals [9], electron transport in semiconductors [10], acoustic wave propagation [11], and molecular orientational relaxation processes [12]. A schematic of the experiment is shown in Fig. 1. Two time coincident picosecond infrared ($\lambda = 4.1\,\mu m$) pulses are crossed in the diamond sample at an angle θ. The two beams produce a sinusoidal interference pattern in the sample with a fringe spacing of $d = \lambda/2\sin(\theta/2)$. Absorption of the infrared light by the two-phonon modes in diamond deposits heat into the sample in a pattern mimicking the original optical interference pattern. The spatially periodic heating of the sample ($\Delta T \approx 0.1\,K$) causes a spatial modulation of the real part of the index of refraction. This produces a diffraction grating. A third, time-delayed probe pulse ($\lambda = 611\,nm$) is diffracted off the grating at the Bragg angle. The probe monitors the decay of the grating as heat diffuses from the peaks to the nulls. The probe diffraction efficiency, η, can be obtained by solution of a one dimensional diffusion equation, and is

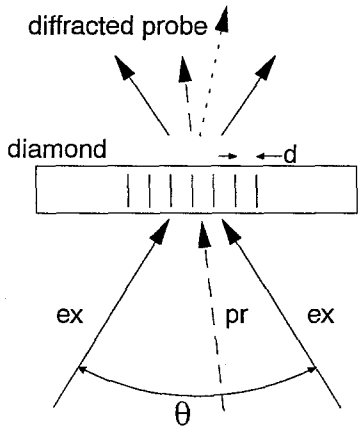

Fig. 1. A schematic of the infrared transient grating experiment. Two excitation pulses (ex) with a wavelength of 4.1 μm are crossed at an angle θ in the diamond. Absorption and rapid relaxation by the two-phonon bands create a thermal grating with fringe spacing, d. The diffraction of a variably delayed probe pulse (pr) monitors the decay of the grating by thermal diffusion from the peaks to the nulls

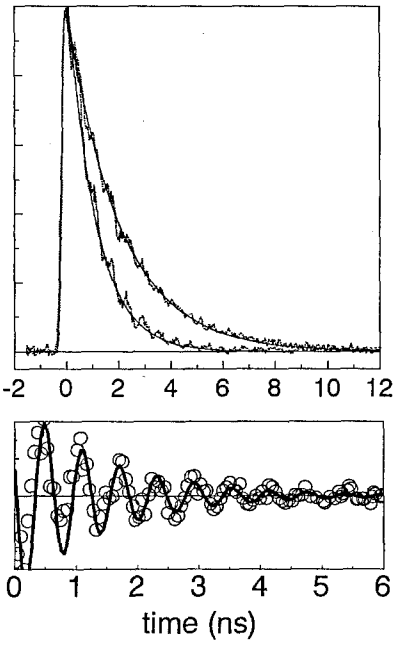

Fig. 2. a Two transient grating decays and exponential fits for natural abundance ^{12}C (*top*) and isotopically enriched diamond (*bottom*), at a fringe spacing of 11.8 μm. **b** An enlargement of the acoustic portion of the signal for the bottom curve in **a** with an exponentially damped sinusoidal fit

given by [8]

$$\eta \propto \exp(-2\alpha\beta^2 t) = \exp(-t/\tau)\,, \tag{1}$$

where $\beta = 2\pi/d$ is the grating wave-vector and $1/\tau$ is the measured grating decay constant. The factor of two arises because the signal intensity in this four-wave mixing experiment is proportional to the square of the induced polarization. Equation (1) shows that the measured exponential grating decay time gives the thermal diffusivity directly from $\alpha = (-2\beta^2\tau)^{-1}$. An accurate test of the diffusive nature of the decay is to vary the grating fringe spacing. This changes the grating wave vector, and the experimental decay time, but the thermal diffusivity remains the same.

Picosecond pulses with a wavelength of 4.1 μm are generated with a $LiIO_3$ optical parametric amplifier (OPA). The pulse train of a cw-pumped, Q-switched, mode-locked, cavity-dumped Nd:YAG laser with a 10% output coupler is doubled and synchronously pumps a sulforhodamine-640 dye laser. The dye laser is cavity dumped simultaneously with the Nd:YAG. The cavity dumped pulse of the Nd:YAG is doubled (532 nm, 80 ps, 800 μJ) and cylindrically down-collimated to a 2 mm × 1 mm beam. The dye-laser pulse (611 nm, 50 ps, 15 μJ) is down-collimated to a 1 mm diameter beam. The two pulses are made time coincident and collinear, and mixed in a 30 mm long $LiIO_3$ crystal (cut 22.5° off optic axis). The beams are combined in the crystal so that the 532 nm beam walks off in the long direction of the cylindrical spot, maximizing the interaction length with the dye beam. The OPA gives 2 μJ, 50 ps pulses at 4.1 μm with a 1 kHz repetition rate.

The three colors are dispersed in a CaF Brewster prism. The 4.1 μm beam is collimated and split into two excitation pulses. The dye beam is spatially filtered and sent through a optical delay, giving it up to 16 ns of delay behind the excitation pulses. The beams are combined in the sample with a 114 mm off-axis parabolic reflector. The 4.1 μm and dye beams are focused to 150 μm and 100 μm at the sample, respectively. The fringe spacing was varied from 11 μm to 20 μm. The excitation beams are chopped at 500 Hz, and the diffracted grating signal is detected by a PMT with a lock-in amplifier.

The grating fringe spacing is determined by the acoustic grating signal from a 10% deuterated ethanol (EtOD) in ethanol. The excitation pulses are absorbed by the EtOD hydrogen-bonded O–H stretching mode, which rapidly relaxes (~1 ps) into phonon modes. This rapid heating launches counterpropagating acoustic waves, with a wavelength equal to the grating fringe spacing. Since the thermal decay is slow relative to the acoustic period, the grating signal probes the density modulations as the acoustic waves travel against each other at the speed of sound. The fringe spacing can be accurately determined by fitting the acoustic grating signal to the speed of sound in ethanol [11]. This method improves on the accuracy of the fringe spacing obtained by direct measurement of the angle between the excitation beams.

Thermal diffusivity measurements were made on two type-IIA synthetic diamond samples, with dimensions 4 mm × 4 mm × 0.5 mm, and ^{12}C isotopic concentrations of 99.9% and 98.9% [14]. A typical transient grating signal decay at room temperature for both samples at a fringe spacing of 11.8 μm is shown in Fig. 2a. The thermal grating decays are exponential over several factors of e, and are also modulated by counterpropagating acoustic waves. The acoustic signal is separated by subtracting the exponential fit to the thermal portion from the signal, taking into account the quadratic dependence of the signal. It can then be fit to an exponentially damped sinusoidal signal, as shown in Fig. 2b. The velocity of sound in diamond, v, determined

by the average to several fits, was $\nu = 1.73 \times 10^6$ cm/s, corresponding to literature values, within 2% [15].

2 Results and Discussion

Measurements of the thermal diffusivity on any spot on the sample were reproducible to within ±1%. However, the thermal diffusivity measurements on both samples varied significantly from point to point over the entire sample. Measurements were made at many points on each sample giving thermal diffusivity values that varied by up to 50% from point to point. To make a determination of the average thermal diffusivity of the samples, measurements were made for several points and averaged. This averaging was then repeated for several fringe spacings. From (1), a plot of the decay constant versus the square of the grating wave vector should give a straight line through the origin with slope of α. Any other effects, such as excited-state contribution to the decay, would result in a non-zero intercept. Figure 3 shows such a plot for fringe spacings of 11.8 μm to 18.0 μm for both natural abundance and isotopically enriched diamond. The slope of the lines give the thermal diffusivity of diamond as 7.8(2) cm^2/s for 98.9% ^{12}C (natural abundance), and 12.0(2) cm^2/s for 99.9% ^{12}C, corresponding to thermal conductivities of 14.0 W/cm K and 21.5 W/cm K, respectively. These results confirm previous measurements of 50% enhancement in the thermal conductivity of isotopically enhanced diamond.

The local variation of the thermal diffusivity is not surprising, when comparing results with X-ray topographs of the samples. X-ray topographs of the samples used in this experiment, published elsewhere [14], show considerable defect structures on the order of ≤100 μm in some regions and relatively few defects in others. In addition, the isotopically enriched sample has substantially less defect structure than the natural abundance sample. This should not influence the results of these measurements as long as the defects exist on a scale long compared to phonon mean free path. At room temperature the phonon mean free path, Λ, calculated from $\Lambda = 3k/\nu C_p$, is $\Lambda \approx 0.2$ μm. It should be noted that the contribution of lattice vacancies to phonon scattering is orders of magnitude greater than isotopic impurities [2].

The values measured for the thermal diffusivity are both approximately 50% less than previously reported values for single-crystal type-IIA diamonds [1, 2, 16]. The value for natural abundance ^{12}C diamond is similar to that reported for type-IA CVD diamond thin films, most of which have crystallite structure on the order of 1–100 μm [3, 4, 6]. The difference between these results and past measurements may be due to the nature of the samples; yet it seems unlikely that both samples would give reduced thermal diffusivities.

The variety of internal checks on the experimental data makes it most reliable. The results obtained are independent of fringe spacing, which demonstrates the diffusive nature of the signal. The onset of acoustic waves at time $t = 0$ demonstrates a rapid relaxation of the initially excited phonons and onset of thermal expansion. The acoustic waves also act as an internal check of the fringe spacing, since they match the velocity of sound in diamond. In addition, the same results are obtained when the intensity of the excitation pulses were cut by half. An experimental inaccuracy, systematic or random, does not seem to be an explanation for the differences between these measurements and previous reports. One possible explanation for differing results involves the initial conditions in these experiments. It is possible that the relaxation of the initially excited two-phonon mode does not produce a thermal distribution of longitudinal acoustic phonons. A bottleneck could trap phonons in the upper part of the acoustic dispersion, resulting in the diffusion of non-equilibrium phonons. This phenomena can be tested by tuning the grating excitation wavelength to a variety of well-defined two-phonon transitions between 3.7 μm and 5.8 μm [13]. In addition to the wavelength studies, a temperature dependent study will give greater information on the phonon mean free path and thus the nature of any defect structure in the samples. Also, these results will be compared to those obtained from other synthetic diamonds as well as natural type-IIA gems.

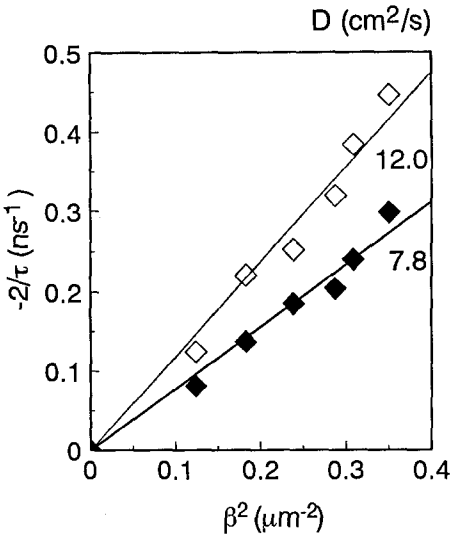

Fig. 3. The plot of the average grating decay constant vs the square of the grating wave vector at six fringe spacings for both diamond samples. The top line corresponds to the isotopically enhanced diamond, and the bottom line to the natural abundance diamond. The intercept at the origin is a check of the diffusive nature of the process

Acknowledgements. The authors gratefully acknowledge Professor T. H. Geballe of the Department of Applied Physics at Stanford University and Dr. Hans Coufal of the IBM Almaden Research Center, San Jose, CA for informative discussions. This work was supported by the National Science Foundation, Division of Materials Research (DMR90-22675) and by the Office of Naval Research, Physics Division (N00014-89-J1119).

References

1. T.R. Anthony, W.F. Banholzer, J.F. Fleischer, L. Wei, P.K. Kuo, R.L. Thomas, R.W. Pryor: Phys. Rev. B **42**, 1104 (1990)
2. D.G. Onn, A. Witek, Y.Z. Qiu, T.R. Anthony, W.F. Banholzer: Phys. Rev. Lett. **68**, 2806 (1992)
3. D.T. Morelli, C.P. Beetz, T.A. Perry: J. Appl. Phys. **64**, 3063 (1988)

4. T.R. Anthony, J.L. Fleischer, J.R. Olson, D.G. Cahill: J. Appl. Phys. **69**, 8122 (1991)
5. E.P. Visser, E.H. Versteegen, W.J.P. van Enckevort: J. Appl. Phys. **71**, 3238 (1992)
6. G. Lu, W.T. Swann: Appl. Phys. Lett. **59**, 1556 (1991)
7. Z. Chen, A. Mandelis, P.G. Kosky: Submitted to Phys. Rev. B (1992)
8. C.D. Marshall, I.M. Fishman, R.C. Dorfman, C.B. Eom, M.D. Fayer: Phys. Rev. B **45**, 10009 (1992)
9. T.S. Rose, R. Righini, M.D. Fayer: Chem. Phys. Lett. **106**, 13 (1984)
10. J.J. Kasinski, L. Gomez-Jahn, L. Min, Q. Bao, R.J.D. Miller: J. Lumin. **40–41**, 555 (1988)
11. M.D. Fayer: IEEE J. QE-**22**, 1437 (1986)
12. P.D. Hyde, T.E. Evert, M.D. Ediger: J. Chem. Phys. **93**, 2274 (1990)
13. C.A. Klein, T.M. Hartnett, C.J. Robinson: Phys. Rev. B **45**, 12854 (1992)
14. T.R. Anthony, W.F. Banholzer: Diamond and Related Materials **1**, 717 (1992)
15. W. Banholzer, T. Anthony, R. Gilmore: *New Diamond Science and Technology* (Materials Research Society, Pittsburgh, PA 1991) p. 857
16. L. Wei, P.K. Kuo, R.L. Thomas, T.R. Anthony, W.F. Banholzer: *New Diamond Science and Technology* (Materials Research Society, Pittsburgh, PA 1991) p. 875